Neural adaptive chaotic control with constrained input using state and output feedback*

Gao Shi-Gen(高士根)[a], Dong Hai-Rong(董海荣)[a]†, Sun Xu-Bin(孙绪彬)[b], and Ning Bin(宁 滨)[a]

[a] *State Key Laboratory of Rail Traffic Control and Safety, Beijing Jiaotong University, Beijing* 100044, *China*
[b] *School of Electronic and Information Engineering, Beijing Jiaotong University, Beijing* 100044, *China*

(Received 16 May 2014; revised manuscript received 28 June 2014; published online 25 November 2014)

This paper presents neural adaptive control methods for a class of chaotic nonlinear systems in the presence of constrained input and unknown dynamics. To attenuate the influence of constrained input caused by actuator saturation, an effective auxiliary system is constructed to prevent the stability of closed loop system from being destroyed. Radial basis function neural networks (RBF-NNs) are used in the online learning of the unknown dynamics, which do not require an off-line training phase. Both state and output feedback control laws are developed. In the output feedback case, high-order sliding mode (HOSM) observer is utilized to estimate the unmeasurable system states. Simulation results are presented to verify the effectiveness of proposed schemes.

Keywords: chaotic control, neural adaptive control, constrained input

PACS: 05.45.Gg **DOI:** 10.1088/1674-1056/24/1/010501

1. Introduction

In recent years, chaotic control has aroused considerable concern after the findings of Lorenz system,[1] Rössler system,[2], Chua system,[3] Sprott system,[4] Chen system,[5] and Lü system.[6] The chaotic control problem was first considered in Ref. [7]. In the following decades, many advanced control methods were reported, such as impulsive control,[8–10] adaptive-dynamic-programming-based optimal control,[11,12] $\mathcal{H}_\infty$ synchronization,[13–15] passive control,[16,17] backstepping,[18,19] and so on. The methods mentioned above were developed based on the assumption that the control signals can be implemented by the serving actuator. However, physical constraints exist widely in every practical control system, that is, it is impossible to implement unlimited control signal in applications, known as the saturation nonlinearity phenomenon.

In Ref. [20], a feedback linearization control is applied to control a chaotic pendulum system considering the presence of saturation in control signals, the stability of the controller is investigated in the presence of saturation, and corresponding sufficient stability conditions are obtained. In Ref. [21], an adaptive sliding mode control scheme for Lorenz chaos subject to saturating input is presented. In Ref. [22], backstepping-based adaptive fuzzy neural controller control of unknown chaotic systems with input saturation is given, the auxiliary system with the same order as that of the plant[23] is used to deal with saturation. It is noticeable that the methods in these works are developed using available system states, which may restrict the real applications in practical engineering in which sometimes only system output information is available for control design. Furthermore, the method in Ref. [23] suffers from the problem of "explosion of complexity", which is caused by the repeated differentiations of the so-called "virtual" controls. Although dynamic surface control technique[24] can be used to solve this difficult point, the backstepping design requires tedious and complex analysis.[25] As reported in Ref. [26], direct current motor control is a relatively simple application, but the regression matrix in the adaptive backstepping control almost covers an entire page in Ref. [27].

In this paper, neural adaptive control is developed for a class of chaotic nonlinear systems subject to unknown dynamics and constrained input. Radial basis function neural networks (RBF-NNs) are used to online approximate unknown nonlinear dynamics, the auxiliary system similar to Refs. [22] and [23] is used to generate signals which attenuate the effect of input saturation. The new features of the developed methods compared to Refs. [22] and [23] contain two aspects: (i) by virtue of properly selected state vector and constructed auxiliary system, backstepping used in Ref. [22]) is not used in this paper; (ii) both state and output feedback cases are considered in this paper. In the output feedback case, HOSM observer[31] is utilized to estimate the unmeasurable system states. The prominent feature of the HOSM observer lies in that it guarantees finite-time observer error convergence and therefore is an admirable tool for feedback control design with separation principle trivially satisfied.

*Project supported by the National High Technology Research and Development Program of China (Grant No. 2012AA041701), the Fundamental Research Funds for Central Universities of China (Grant No. 2013JBZ007), the National Natural Science Foundation of China (Grant Nos. 61233001, 61322307, 61304196, and 61304157), and the Research Program of Beijing Jiaotong University, China (Grant No. RCS2012ZZ003).

†Corresponding author. E-mail: hrdong@bjtu.edu.cn

© 2015 Chinese Physical Society and IOP Publishing Ltd

2. Problem formulation and preliminaries

Consider a class of uncertain chaotic systems in the following form:

$$\begin{cases} \dot{x}_i = x_{i+1}, \quad (i = 1, 2, \ldots, n-1), \\ \dot{x}_n = f(\bar{\boldsymbol{x}}) + v, \\ y = x_1, \end{cases} \tag{1}$$

where $\bar{\boldsymbol{x}} = [x_1, x_2, \ldots, x_n]^{\mathrm{T}}$ is the state vector, $f(\cdot)$ is an unknown smooth nonlinear function, y is the output, v is the output of serving actuator, which holds the nonlinear relationship with designed control input u in the following form:

$$v = \begin{cases} \mathrm{sign}(u)u^+, & \text{if } |u| > u^+, \\ u, & \text{otherwise}, \end{cases} \tag{2}$$

where u^+ denotes the bound of the serving actuator.

The objective is to design a proper control u such that: (i) the closed-loop system is semi-globally stable in the sense that all the signals are ultimately uniformly bounded; (ii) the output of chaotic system $y = x_1$ tracks the desired signal y_{r} with adjustable tracking error.

To this end, the following lemma and assumptions are used to design a feasible control law.

Lemma 1[33] An unknown smooth function $\boldsymbol{F}(\boldsymbol{Z})$ can be approximated by RBF NNs as $\boldsymbol{F}(\boldsymbol{Z}) = \boldsymbol{W}^{\mathrm{T}}\boldsymbol{S}(\boldsymbol{Z})$, where $\boldsymbol{Z} \in \boldsymbol{\Omega}_Z \subset \boldsymbol{R}^q$ is the input to the neural network, with q being the NN input dimension, $\boldsymbol{W} = [w_1, w_2, \ldots, w_l]^{\mathrm{T}}$ is the adjustable parameters vector, l is the number of neurons, $\boldsymbol{S}(\boldsymbol{Z}) = [s_1(\boldsymbol{Z}), s_2(\boldsymbol{Z}), \ldots, s_l(\boldsymbol{Z})]^{\mathrm{T}}$, with $s_i(Z)$ being Gaussian functions, i.e., $s_i(\boldsymbol{Z}) = \exp(-(\boldsymbol{Z} - \mu_i)^{\mathrm{T}}(\boldsymbol{Z} - \mu_i)/\eta_i^2)$, $i = 1, 2, \ldots, l$, where μ_i and η_i denote the centers and widths of the Gaussian functions, respectively. As indicated in Ref. [34], by setting a large enough number of hidden neurons, the RBF NNs are capable of approximating $\boldsymbol{F}(\boldsymbol{Z})$ to arbitrary accuracy over a compact set $\boldsymbol{\Omega}_Z \subset \boldsymbol{R}^q$

$$\boldsymbol{F}(\boldsymbol{Z}) = \boldsymbol{W}^{*\mathrm{T}}\boldsymbol{S}(\boldsymbol{Z}) + \varepsilon(\boldsymbol{Z}),$$

where $\boldsymbol{W}^*$ is the so-called "optimal" bounded weight vector which minimizes $\varepsilon(\boldsymbol{Z})$

$$\boldsymbol{W}^* := \arg \min_{\boldsymbol{W} \in \mathbb{R}^l} \left\{ \sup_{\boldsymbol{Z} \in \boldsymbol{\Omega}_Z} |\boldsymbol{F}(\boldsymbol{Z}) - \boldsymbol{W}^{\mathrm{T}}\boldsymbol{S}(\boldsymbol{Z})| \right\},$$

with $\varepsilon(\boldsymbol{Z})$ being the bounded approximation error, and $|\varepsilon(\boldsymbol{Z})| \leq \varepsilon^*$.

Assumption 1 The optimal neural weight vector $\boldsymbol{W}^*$ is bounded by unknown constant $\|\boldsymbol{W}^*\| \leq \boldsymbol{W}^+$, and $\boldsymbol{W}^+ > 0$ is an unknown constant. The Gaussian basis function vector $\boldsymbol{S}(\boldsymbol{Z})$ is also bounded, i.e., $\|\boldsymbol{S}(\boldsymbol{Z})\| \leq \boldsymbol{S}^*$ with $S^* > 0$ being an unknown constant.

Assumption 2 The desired signal y_{r} and its derivatives up to the n-th order are known and bounded.

Assumption 3[36] The system (1) is input-to-state stable.

Remark 1 As indicated in Ref. [35], it is extremely hard to obtain general stability conditions for general unstable systems with input saturation. Therefore, Assumption 3 is used in Ref. [36] to develop feasible control law. In this paper, Assumption 3 implies that the chaotic systems considered are stable, since the actual input to the system is always bounded by saturation, the boundedness of states are guaranteed, which will facilitate the stability analysis in the following analysis.

3. Control design

3.1. Neural adaptive control using state feedback

Define the following vectors:

$$\begin{aligned} \bar{\boldsymbol{x}} &= [x_1, x_2, \ldots, x_n]^{\mathrm{T}} \in \boldsymbol{R}^n, \\ \bar{\boldsymbol{y}}_{\mathrm{r}} &= [y_{\mathrm{r}}, \dot{y}_{\mathrm{r}}, \ldots, y_{\mathrm{r}}^{(n-1)}]^{\mathrm{T}} \in \boldsymbol{R}^n, \\ \boldsymbol{e} &= \bar{\boldsymbol{x}} - \bar{\boldsymbol{y}}_{\mathrm{r}} - \boldsymbol{\zeta}, \end{aligned}$$

where $\boldsymbol{\zeta} \in \boldsymbol{R}^n$ is an auxiliary signal vector generated by the following constructed system:

$$\dot{\boldsymbol{\zeta}} = -\begin{bmatrix} \kappa_1 & -1 & & & \\ & \kappa_2 & -1 & & \\ & & \ddots & \ddots & \\ & & & \ddots & -1 \\ & & & & \kappa_n \end{bmatrix} \boldsymbol{\zeta} + \begin{bmatrix} 0 \\ 0 \\ \vdots \\ 0 \\ 1 \end{bmatrix} \Delta \boldsymbol{u}, \tag{3}$$

where $\kappa_1, \kappa_2, \ldots, \kappa_n$ are design parameters, and $\Delta u := v - u$.

Remark 2 By setting the initial value of $\boldsymbol{\zeta}$ as 0, the auxiliary system given in Eq. (3) has no response without input saturation, i.e., $\Delta \boldsymbol{u} = 0$. When saturation happens, a sudden rise will appear in $\bar{\boldsymbol{x}} - \bar{\boldsymbol{y}}_{\mathrm{r}}$ because there is not enough input effort available to make $\bar{\boldsymbol{x}} - \bar{\boldsymbol{y}}_{\mathrm{r}}$ zero. At the same time, the auxiliary signal $\boldsymbol{\zeta}$ will increase to reduce the amplitude of $\boldsymbol{e}$, i.e., adaptation rate is lowered with input saturation in effect. After saturation terminates, $\Delta \boldsymbol{u} = 0$, $\boldsymbol{\zeta}$ will decay to zero, that is, there is no supererogatory computation without saturation. This is the working mechanism of Eq. (3) to attenuate the effect introduced by constrained input.

Introduce a filtered tracking error as follows:

$$\mathcal{S} = [\boldsymbol{\Lambda}^{\mathrm{T}}\ 1]\boldsymbol{e}, \tag{4}$$

where $\boldsymbol{\Lambda} = [\lambda_1, \lambda_2, \ldots, \lambda_{n-1}]^{\mathrm{T}}$, λ_i $(i = 1, 2, \ldots, n-1)$ are chosen such that the polynomial $s^{n-1} + \lambda_{n-1}s^{n-2} + \ldots + \lambda_1$ is Hurwitz. In this sense, one can guarantee boundedness of $\boldsymbol{e}$ with bounded $\mathcal{S}$.

The designed neural adaptive control for chaotic system described by Eq. (1) is given in the following theorem.

Theorem 1 Consider the chaotic system described by Eq. (1). If a neural adaptive control with weight adaptation laws are designed as follows:

$$\boldsymbol{u} = -\left(k_1 + \frac{1}{2}\right)\mathcal{S} - \hat{\boldsymbol{W}}_1^{\mathrm{T}}\boldsymbol{S}(\boldsymbol{Z}) + \boldsymbol{y}_{\mathrm{r}}^{(n)} - [\boldsymbol{\Lambda}^{\mathrm{T}}\ 1]\boldsymbol{K}\boldsymbol{\zeta},$$

$$\dot{\hat{\boldsymbol{W}}}_1 = \boldsymbol{\Gamma}_1(\boldsymbol{S}(\boldsymbol{Z})\mathcal{S} - \sigma_1\hat{\boldsymbol{W}}_1), \tag{5}$$

where $k_1 > 0$ is a design parameter, $\boldsymbol{K} = \mathrm{diag}\{\kappa_1, \kappa_2, \ldots, \kappa_n\}$ is a diagonal matrix, where $\kappa_1, \kappa_2, \ldots, \kappa_n$ are design parameters defined in Eq. (3). $\boldsymbol{\Gamma}_1 = \boldsymbol{\Gamma}_1^{\mathrm{T}} > 0$ is adaptive gain matrix, $\hat{\boldsymbol{W}}_1$ is the estimated value of $\boldsymbol{W}_1^*$, $\sigma_1 > 0$ is a small constant introduced as σ modification[28] to prevent the estimated value $\hat{\boldsymbol{W}}_1$ from drifting to be very large. Then,

(i) All the signals in the closed-loop system are uniformly ultimately bounded.

(ii) The transient performance of tracking error between system output y and reference signal y_{r} with input saturation in effect satisfies the following inequalities:

$$|\mathcal{S}| \leq \sqrt{\frac{2\tau_2}{\tau_1} + 2V_1(0)}, \quad |\zeta| \leq \frac{\Delta u}{\Pi_{k=1}^n \kappa_k},$$

where

$$\tau_1 := \frac{\min\{k_1, \sigma_1/2\}}{\max\{1/2, \|\Gamma_1^{-1}\|/2\}}$$

and

$$\tau_2 := \frac{1}{2}\varepsilon^2 + \frac{1}{2}\sigma_1\|W_1^*\|^2,$$

and $V_1(0)$ is the initial value of $V_1(t)|_{t=0}$.

Proof Considering the open-loop dynamics (4) and control laws (5), the closed-loop dynamics is obtained as

$$\begin{aligned}\dot{\mathcal{S}} &= [0\ \Lambda^{\mathrm{T}}]\boldsymbol{e} + \boldsymbol{f}(\bar{\boldsymbol{x}}) - \boldsymbol{y}_{\mathrm{r}}^{(n)} + \boldsymbol{u} + [\Lambda^{\mathrm{T}}\ 1]\boldsymbol{K}\boldsymbol{\zeta} \\ &= -\left(\boldsymbol{k}_1 + \frac{1}{2}\right)\mathcal{S} + [0\ \Lambda^{\mathrm{T}}]\boldsymbol{e} + \boldsymbol{f}(\bar{\boldsymbol{x}}) - \hat{\boldsymbol{W}}_1^{\mathrm{T}}\boldsymbol{S}(\boldsymbol{Z}),\end{aligned} \tag{6}$$

where $\hat{\boldsymbol{W}}_1^{\mathrm{T}}\boldsymbol{S}(\boldsymbol{Z})$ is utilized to approximate the unknown nonlinear function $[0\ \Lambda^{\mathrm{T}}]\boldsymbol{e} + \boldsymbol{f}(\bar{\boldsymbol{x}})$, and $\hat{\boldsymbol{W}}_1$ is the estimated value of optimal weight vector $\boldsymbol{W}_1^*$.

Consider the following Lyapunov candidate:

$$\boldsymbol{V}_1 = \frac{1}{2}\mathcal{S}^2 + \frac{1}{2}\tilde{\boldsymbol{W}}_1^{\mathrm{T}}\boldsymbol{\Gamma}_1^{-1}\tilde{\boldsymbol{W}}_1, \tag{7}$$

its derivative along the adaptation laws can be calculated by

$$\begin{aligned}\dot{V}_1 &= -\left(k_1 + \frac{1}{2}\right)\mathcal{S}^2 + \mathcal{S}\tilde{\boldsymbol{W}}_1^{\mathrm{T}}\boldsymbol{S}(\boldsymbol{Z}) + \mathcal{S}\varepsilon + \tilde{\boldsymbol{W}}_1^{\mathrm{T}}\Gamma_1^{-1}\dot{\hat{\boldsymbol{W}}}_1 \\ &= -\left(k_1 + \frac{1}{2}\right)\mathcal{S}^2 + \mathcal{S}\varepsilon + \sigma_1\tilde{\boldsymbol{W}}_1^{\mathrm{T}}\hat{\boldsymbol{W}}_1 \\ &\leq -k_1\mathcal{S}^2 - \frac{1}{2}\sigma_1\tilde{\boldsymbol{W}}_1^{\mathrm{T}}\tilde{\boldsymbol{W}}_1 + \frac{1}{2}\varepsilon^2 + \frac{1}{2}\sigma_1\|\boldsymbol{W}_1^*\|^2.\end{aligned} \tag{8}$$

Define $\tau_1 = \min\{k_1, \sigma_1/2\}/\max\{1/2, \|\Gamma_1^{-1}\|/2\}$ and $\tau_2 = \frac{1}{2}\varepsilon^2 + \frac{1}{2}\sigma_1\|\boldsymbol{W}_1^*\|^2$, then $\dot{\boldsymbol{V}}_1 \leq -\tau_1\boldsymbol{V}_1 + \tau_2$. Furthermore, we have $0 \leq \boldsymbol{V}_1(t) \leq \tau_2/\tau_1 + \mathrm{e}^{-\tau_1 t}(V_1(0) - \tau_2/\tau_1)$. Based on the definition of V_1, it follows

$$|\mathcal{S}| \leq \sqrt{\frac{2\tau_2}{\tau_1} + 2\mathrm{e}^{-\tau_1 t}\left(V_1(0) - \frac{\tau_2}{\tau_1}\right)},$$

$$\|\tilde{\boldsymbol{W}}_1\| \leq \sqrt{\frac{2}{\|\Gamma_1^{-1}\|}\left[\frac{\tau_2}{\tau_1} + \mathrm{e}^{-\tau_1 t}\left(V_1(0) - \frac{\tau_2}{\tau_1}\right)\right]},$$

implying that there exists a moment T such that for any $t > T$, one has

$$|\mathcal{S}| \leq \sqrt{\frac{2\tau_2}{\tau_1} + 2V_1(0)},$$

$$\|\tilde{\boldsymbol{W}}_1\| \leq \sqrt{\frac{2}{\|\Gamma_1^{-1}\|}\left(\frac{\tau_2}{\tau_1} + V_1(0)\right)}.$$

When the input saturation is in effect, the solution of Eq. (3) can be obtained as $|\zeta| \leq \Delta u/\prod_{k=1}^n \kappa_k$. Based on Eq. (4), it is known that $\boldsymbol{e}$ is bounded. In view of Assumption 3, the $\bar{\boldsymbol{x}}$ is bounded in that system input is always bounded by saturation, which further guarantees the boundedness of $\boldsymbol{\zeta}$. Therefore, $\boldsymbol{u}$ and $\Delta\boldsymbol{u}$ are bounded. All the signals in the closed-loop system are bounded. The proof is completed.

3.2. Neural adaptive control using output feedback

In this section, neural adaptive control is designed using output feedback, i.e., only y can be used in the control design. To this end, a high-order sliding mode observer named Levant's differentiator is utilized, as described in the following lemma.

Lemma 2[31] *Levant's differentiator* Consider a signal $\mathcal{L}(t)$ defined in the range of $[0, \infty]$, which is composed of a bounded noise and an unknown base signal $\mathcal{L}_0(t)$, with the noise being Legesgue measurable and the n-th derivative of base signal $\mathcal{L}_0(t)$ having a known Lipschitz constant $L > 0$. The following constructed high-order sliding mode observer, with β_i $(i = 1, 2, \ldots, n)$ being positive constants selected by the designers:

$$\begin{cases} \dot{\hat{x}}_1 = p_1, \\ p_1 = -\beta_1|\hat{x}_1 - \mathcal{L}(t)|^{\frac{n}{n+1}}\mathrm{sign}(\hat{x}_1 - \mathcal{L}(t)) + \hat{x}_2, \\ \dot{\hat{x}}_i = p_i, \\ p_i = -\beta_i|\hat{x}_i - p_{i-1}|^{\frac{n-i+1}{n-i+2}}\mathrm{sign}(\hat{x}_i - p_{i-1}) + \hat{x}_{i+1}, \\ \qquad i = 2, 3, \ldots, n, \\ \dot{\hat{x}}_{n+1} = -\beta_{n+1}\mathrm{sign}(\hat{x}_{n+1} - p_n), \end{cases} \tag{9}$$

guarantees that (i) there exists a time moment T, such that for any $t > T$, one obtains $\hat{x}_i(t) = \mathcal{L}_0^{(i-1)}(t)$, $i = 1, 2, \ldots, n+1$ in the absence of input noise by choosing proper β_i, $i = 1, 2, \ldots, n$. Furthermore, the solutions of Eq. (9) are finite-time stable based on Ref. [31]; (ii) if a bounded noise satisfying $|\mathcal{L}(t) - \mathcal{L}_0(t)| \leq \varepsilon$ exists, then $|\hat{x}_i(t) - \mathcal{L}_0^{(i-1)}| \leq \varsigma_i\varepsilon^{\frac{n-i+2}{n+2}}$, $i = 1, 2, \ldots, n+1$, $|p_i - \mathcal{L}_0^{(i)}(t)| \leq \mu_i\varepsilon^{\frac{n-i+1}{n+2}}$, $i = 1, 2, \ldots, n$, where ς_i and μ_i are positive constants depending exclusively on the parameters of Eq. (9).

Remark 3 Lemma 2 means that equation (9) is kept in two-sliding mode, i.e., $\hat{\boldsymbol{x}}$ can achieve precise estimation of x in finite time. It is clear that the observer error will converge to a small bounded region which is associated with the magnitude

of noise in finite time. Therefore, it is reasonable to assume that noise exists when measuring the system output y. In this sense, there is a positive constant ν and a time moment T, such that for any $t > T$, $\|\hat{x} - x\| \leq \nu$.

By virtue of the property of the above-mentioned observers, $\bar{\boldsymbol{x}}$ is estimated by the observer, i.e., estimated value $\hat{\boldsymbol{x}}$ is available in the control design. Define the following vectors:

$$\hat{\boldsymbol{x}} = [\hat{x}_1, \hat{x}_2, \ldots, \hat{x}_n]^{\mathrm{T}} \in \boldsymbol{R}^n,$$
$$\hat{\boldsymbol{e}} = \hat{\boldsymbol{x}} - \bar{\boldsymbol{y}}_{\mathrm{r}} - \boldsymbol{\zeta},$$

therefore, $\hat{\mathcal{S}} = [\boldsymbol{\Lambda}^{\mathrm{T}}\ 1]\hat{\boldsymbol{e}}$, $\tilde{\boldsymbol{x}} = e - \hat{\boldsymbol{e}} = \boldsymbol{x} - \hat{\boldsymbol{x}}$, $\tilde{\mathcal{S}} = \mathcal{S} - \hat{\mathcal{S}} = [\boldsymbol{\Lambda}^{\mathrm{T}}\ 1]\tilde{\boldsymbol{x}}$.

The designed output feedback neural adaptive control using sliding-mode observer is given in the following theorem.

Theorem 2 Consider the chaotic system described by Eq. (1). If a neural adaptive control with weight adaptation laws are designed as follows:

$$\boldsymbol{u} = -\left(k_2 + \frac{1}{2}\right)\hat{\mathcal{S}} - \hat{\boldsymbol{W}}_2^{\mathrm{T}}\boldsymbol{S}(Z) + \boldsymbol{y}_{\mathrm{r}}^{(n)} - [\boldsymbol{\Lambda}^{\mathrm{T}}\ 1]\boldsymbol{K}\boldsymbol{\zeta},$$
$$\dot{\hat{\boldsymbol{W}}}_2 = \Gamma_2(\boldsymbol{S}(\boldsymbol{Z})\hat{\mathcal{S}} - \sigma_2|\hat{\mathcal{S}}|\hat{\boldsymbol{W}}_2), \tag{10}$$

where $k_2 > 0$ is a design parameter, $\boldsymbol{\Gamma}_2 = \boldsymbol{\Gamma}_2^{\mathrm{T}} > 0$ is adaptive gain matrix, $\hat{\boldsymbol{W}}_2$ is the estimated value of $\boldsymbol{W}_2^*$, and $\sigma_2 > 0$.

(i) All the signals in the closed-loop system are uniformly ultimately bounded.

(ii) The transient performance of tracking error between system output $\boldsymbol{y}$ and reference signal $\boldsymbol{y}_{\mathrm{r}}$ with input saturation in effect satisfies the following inequalities:

$$|\mathcal{S}| \leq \sqrt{\frac{2\tau_3}{k_2} + 2V_2(0)}, \quad |\zeta| \leq \frac{\Delta u}{\Pi_{k=1}^n \kappa_k},$$

where $\tau_3 := \frac{1}{2}\epsilon^2$, $\epsilon = \epsilon_1 + \boldsymbol{W}^* + \boldsymbol{S}^*/\sigma_2 + \varepsilon^*$, $\epsilon_1 = (k_2 + \frac{1}{2})\max\{\lambda_1, \ldots, \lambda_{n-1}, 1\}\nu$, and $V_2(0)$ is the initial value of $V_2(t)|_{t=0}$.

Proof Consider a Lyapunov function $V_{\mathrm{w}} = \frac{1}{2\Gamma_2}\hat{\boldsymbol{W}}_2^{\mathrm{T}}\hat{\boldsymbol{W}}_2$. Its time derivative is calculated by

$$\begin{aligned}\dot{V}_{\mathrm{w}} &= \hat{\boldsymbol{W}}_2(\boldsymbol{S}(\boldsymbol{Z})\hat{\mathcal{S}} - \sigma_2|\hat{\mathcal{S}}|\hat{\boldsymbol{W}}_2) \\ &\leq -\|\hat{\boldsymbol{W}}_2\||\hat{\mathcal{S}}|(\sigma_2\|\hat{\boldsymbol{W}}_2\| - \boldsymbol{S}^*).\end{aligned} \tag{11}$$

It is clear that $\dot{\boldsymbol{V}}_{\mathrm{w}} \leq 0$ if $\|\hat{\boldsymbol{W}}_2\| > S^*/\sigma_2$. In view of Lyapunov theorem,[32] $\hat{\boldsymbol{W}}_2$ is bounded by $\|\hat{\boldsymbol{W}}_2\| \leq S^*/\sigma_2$. Therefore, the estimation error $\tilde{\boldsymbol{W}}_2$ is bounded by $\|\tilde{\boldsymbol{W}}_2\| \leq W^+ + S^*/\sigma_2$.

The closed-loop system is governed by

$$\dot{\mathcal{S}} = -\left(k_2 + \frac{1}{2}\right)\hat{\mathcal{S}} + [0\ \boldsymbol{\Lambda}^{\mathrm{T}}]e + \boldsymbol{f}(\bar{\boldsymbol{x}}) - \hat{\boldsymbol{W}}_2^{\mathrm{T}}\boldsymbol{S}(\boldsymbol{Z}), \tag{12}$$

where $\hat{\boldsymbol{W}}_2^{\mathrm{T}}\boldsymbol{S}(\boldsymbol{Z})$ is utilized to approximate the unknown nonlinear function $[0\ \boldsymbol{\Lambda}^{\mathrm{T}}]\boldsymbol{e} + \boldsymbol{f}(\bar{\boldsymbol{x}})$, and $\hat{\boldsymbol{W}}_2$ is the estimated value of optimal weight vector $\boldsymbol{W}_2^*$.

Consider a Lyapunov function $V_2 = \frac{1}{2}\mathcal{S}^2$, its time derivative along Eq. (12) is calculated by

$$\begin{aligned}\dot{\boldsymbol{V}}_2 &= -\left(k_2 + \frac{1}{2}\right)\mathcal{S}\hat{\mathcal{S}} + \mathcal{S}\left(\tilde{\boldsymbol{W}}_2^{\mathrm{T}}\boldsymbol{S}(\boldsymbol{Z}) + \varepsilon(Z)\right) \\ &= -\left(k_2 + \frac{1}{2}\right)\mathcal{S}^2 \\ &\quad + \mathcal{S}\left(\left(k_2 + \frac{1}{2}\right)[\Lambda^{\mathrm{T}}\ 1]\tilde{x} + \tilde{\boldsymbol{W}}_2^{\mathrm{T}}\boldsymbol{S}(\boldsymbol{Z}) + \varepsilon(Z)\right) \\ &\leq -k_2\mathcal{S}^2 + \tau_3,\end{aligned}$$

where $\tau_3 = \frac{1}{2}\varepsilon^2$, $\varepsilon = \varepsilon_1 + W^* + S^*/\sigma_2 + \varepsilon^*$, and $\varepsilon_1 = (k_2 + \frac{1}{2})\max\{\lambda_1, \ldots, \lambda_{n-1}, 1\}\nu$. The remainder of the proof is similar to the proof of Theorem 1, which is not discussed in detail here. The proof is completed.

Remark 4 Since the approximation property of RBF NNs in Lemma 1 is only guaranteed in the compact set specified by Ω_Z, the stability results in this work, therefore, are semi-global. In this sense, a reasonable suggestion, i.e., small sets of initial values of NN weights and tracking error, is made to the ones who want to put the main results of this work into practice.

4. Simulation results

To evaluate the developed algorithms for controlling chaotic systems, we consider two nonlinear chaotic systems, i.e., Duffing system and Arneodo system. To simulate the measurement noise when applying Theorem 2, a random number with proper amplitude is added to the observer input signal in each discrete time computation, which is rough enough to mimic measurement noise. The sample time used in the simulation is $\Delta T = 10^{-4}$, without proper designed control scheme, the amplitude of noise is potentially amplified by 10^4 and 10^8 times for two- and three-order systems in discrete time calculation.

4.1. Duffing system

Consider the following Duffing system,[29] whose chaotic behavior is shown in Fig. 1.

$$\begin{cases}\dot{x}_1 = x_2, \\ \dot{x}_2 = -0.1x_2 - x_1^3 + 12\cos(t).\end{cases} \tag{13}$$

Theorem 1 and Theorem 2 are applied to the Duffing system to control the output to track the reference signal $y_{\mathrm{r}} = \sin(t)$ with constrained input specified by $u^+ = 12$. The design parameters are set as follows: $k_1 = k_2 = 15$, $\kappa_1 = 6$, $\kappa_2 = 8$, $\Lambda = 5$, $\Gamma_1 = \Gamma_2 = I$, and $\sigma_1 = \sigma_2 = 0.001$. The neural networks contain 41 nodes with centers evenly spaced on $[-2, 2]$ and widths are

all 1. Initial values of x_1, x_2, ζ_1, and ζ_2 are 0.6, 0.15, 0, and 0, respectively. Initial values of neural network weights are all 0. The parameters of the HOSM observer are $\beta_1 = 12$, $\beta_2 = 15$, and $\beta_3 = 20$. The noise is added to the observer in the form of $\omega = \alpha \cdot \text{rand}[-0.5, 0.5]$, with $\alpha = 0.01$ in this case.

Simulation results of controlling Duffing system are presented by Figs. 2–6. Figure 2 presents the tracking performance and tracking errors in controlling Duffing system, and the state x_2 of the controlled Duffing system is shown in Fig. 3. Signals generated by constructed auxiliary system are shown in Fig. 4, while figure 5 presents the observer errors using Theorem 2. The boundedness of control inputs are shown in Fig. 6. It is observed that all the closed-loop signals are bounded and the performance is satisfactory.

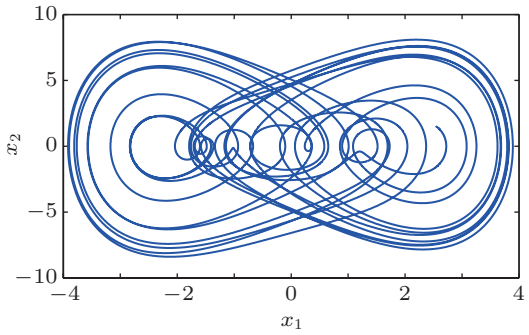


Fig. 1. (color online) Chaotic behavior of Duffing system.

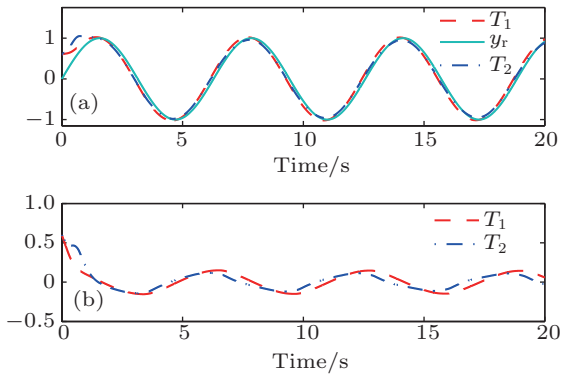


Fig. 2. (color online) (a) Tracking performance of Duffing system (dashed line: output using Theorem 1, solid line: reference signal, dot-dashed line: output using Theorem 2). (b) Tracking errors (dashed line: error using Theorem 1, dot-dashed line: error using Theorem 2).

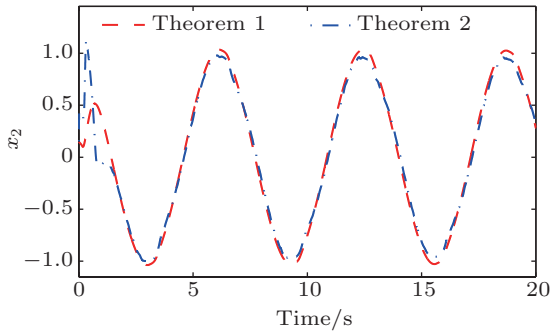


Fig. 3. (color online) State x_2 of controlled Duffing system.

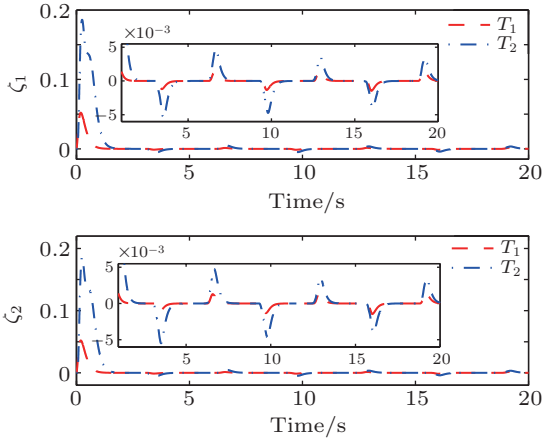


Fig. 4. (color online) Trajectories of (a) ζ_1 and (b) ζ_2.

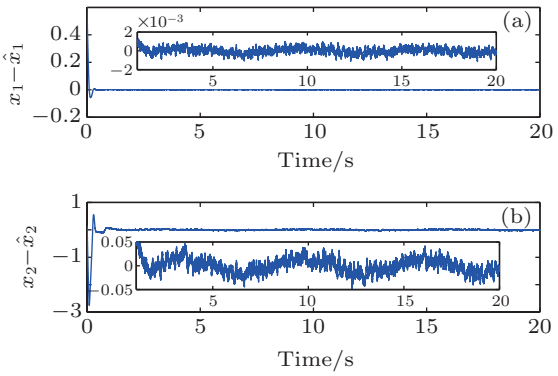


Fig. 5. (color online) Observer errors (a) x_1–$\hat{x}_1$, (b) x_2–$\hat{x}_2$ using Theorem 2.

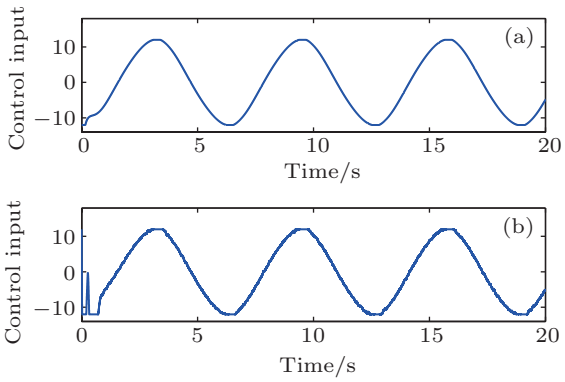


Fig. 6. (color online) Control inputs in controlling Duffing system. (a) Theorem 1; (b) Theorem 2.

4.2. Arneodo system

Consider the following Arneodo system,[30] whose chaotic behavior is shown in Fig. 7.

$$\begin{cases} \dot{x}_1 = x_2, \\ \dot{x}_2 = x_3, \\ \dot{x}_3 = 5.5x_1 - 3.5x_2 - x_3 - x_1^3. \end{cases} \tag{14}$$

The reference signal is also $y_r = \sin(t)$ with $u^+ = 12$. The design parameters here are as follows: $k_1 = k_2 = 5$, $\kappa_1 = 9$, $\kappa_2 = 8$, $\kappa_3 = 7$, $\boldsymbol{\Lambda} = [35\ 12]^{\mathrm{T}}$, $\Gamma_1 = \Gamma_2 = I$, and $\sigma_1 = \sigma_2 = 0.001$. Other settings are the same as the above subsection.

The parameters of the HOSM observer are $\beta_1 = 10$, $\beta_2 = 15$, $\beta_3 = 18$, $\beta_4 = 5$, and $\alpha = 0.001$.

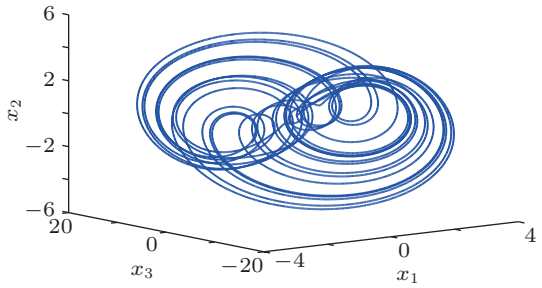


Fig. 7. (color online) Chaotic behavior of Arneodo system.

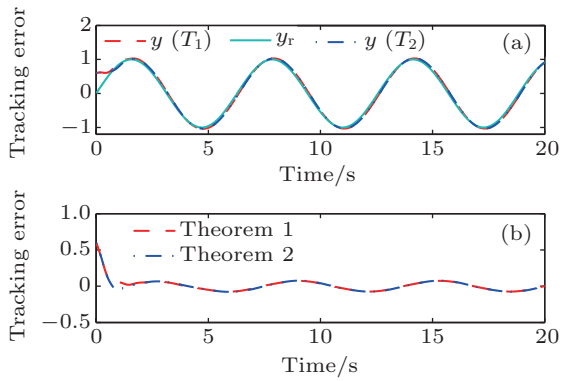


Fig. 8. (color online) (a) Tracking performance of Arneodo system (dashed line: output using Theorem 1, solid line: reference signal, dot-dashed line: output using Theorem 2). (b) Tracking errors (dashed line: error using Theorem 1, dot-dashed line: error using Theorem 2).

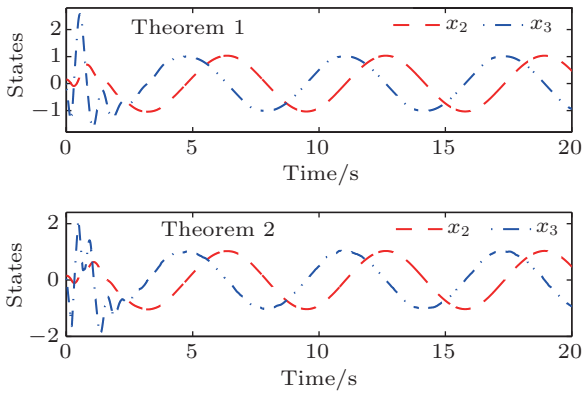


Fig. 9. (color online) States x_2 and x_3 of controlled Arneodo system.

Simulation results of the controlling Arneodo system are presented by Figs. 8–12. Figure 8 presents the tracking performance and tracking errors in controlling Arneodo system, and the states x_2 and x_3 of controlled Arneodo system are shown in Fig. 9. Signals generated by constructed auxiliary system are shown in Fig. 10, while figure 11 presents the observer errors using Theorem 2. The boundedness of control inputs are shown in Fig. 12. Clearly, the tracking performance is satisfactory in controlling Arneodo system as well.

From the aforementioned theoretical analysis and simulation results of both cases, we can conclude that the developed control schemes are valid for a class of uncertain chaotic nonlinear systems with constrained input.

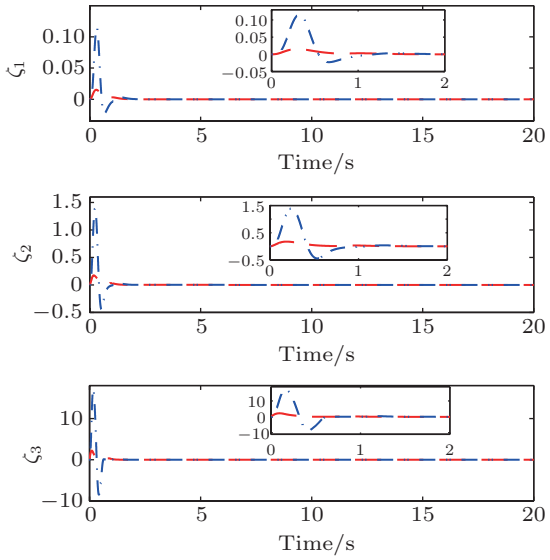


Fig. 10. (color online) Trajectories of (a) ζ_1, (b) ζ_2, and (c) ζ_3.

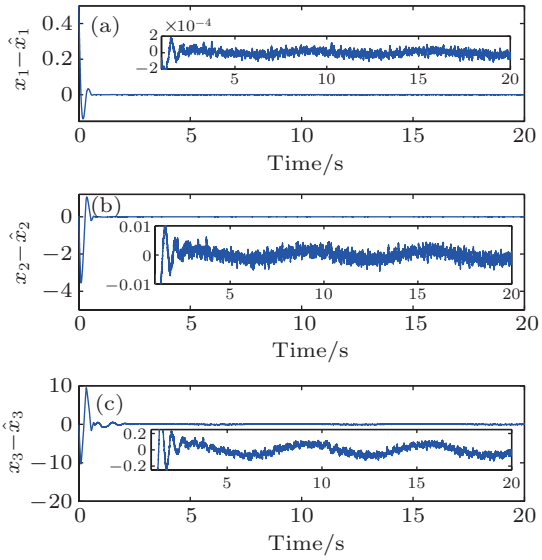


Fig. 11. (color online) Observer errors (a) x_1–$\hat{x}_1$, (b) x_2–$\hat{x}_2$, (c) x_3–$\hat{x}_3$ using Theorem 2.

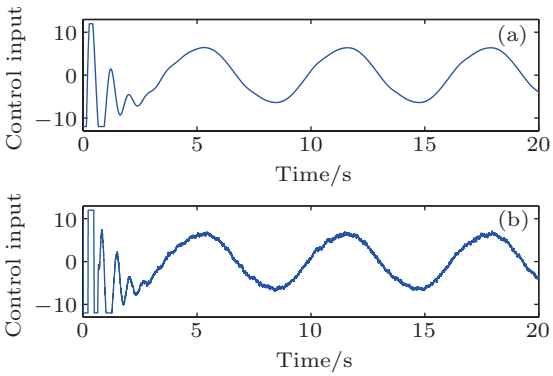


Fig. 12. (color online) Control inputs in controlling Arneodo system. (a) Theorem 1; (b) Theorem 2.

5. Conclusions

This paper has developed neural adaptive control schemes for a class of chaotic nonlinear systems in the presence of constrained input and uncertain dynamics. RBF NNs are used in the online learning of uncertain dynamics. To attenuate the effect caused by constrained input, an auxiliary system with the same order as that of the plant is constructed to generate signals to compensate the effect of input saturation. Except showing the stability of closed-loop system, transient performance with input saturation in effect is obtained rigorously in terms of design parameters. Applications of the developed methods to Duffing system and Arneodo system to track a reference trajectory. Simulation results show that the methods developed perform successful control and achieve desired performance.

References

[1] Lorenz E 1963 *J. Atmos. Ser.* **20** 130
[2] Rössler O E 1976 *Phys. Lett. A* **57** 397
[3] Chua L O, Komuro M and Matsumoto T 1986 *IEEE Trans. Circ. Syst.* **33** 1072
[4] Sprott J C 1994 *Phys. Rev. E* **50** R647
[5] Chen G R and Ueta T 1999 *Int. J. Bifurcation Chaos* **9** 1465
[6] Lü J H and Chen G R 2002 *Int. J. Bifurcation Chaos* **12** 3659
[7] Ott E, Grebogi C and Yorke J A 1990 *Phys. Rev. Lett.* **64** 1196
[8] Ma T and Fu J 2011 *Chin. Phys. B* **20** 050511
[9] Liu D F, Wu Z Y and Ye Q L 2014 *Chin. Phys. B* **23** 040504
[10] Ma T, Zhang H and Fu J 2008 *Chin. Phys. B* **17** 4407
[11] Song R Z, Xiao W D, Sun C Y and Wei Q L 2013 *Chin. Phys. B* **22** 090502
[12] Song R Z, Xiao W D and Wei Q L 2014 *Chin. Phys. B* **23** 050504
[13] Yang D D 2014 *Chin. Phys. B* **23** 010504
[14] Kwon O M, Park M J, Park J H, Lee S M and Cha E J 2013 *Chin. Phys. B* **22** 110504
[15] Fu S H, Lu Q S and Du Y 2012 *Chin. Phys. B* **21** 060507
[16] Zhu D R, Liu C X and Yan B N 2012 *Chin. Phys. B* **21** 090509
[17] Song Y Z, Zhao G Z and Qi D L 2006 *Chin. Phys.* **15** 2266
[18] Yassen M T 2006 *Chaos Soliton. Fract.* **27** 537
[19] Li H Y and Hu Y A 2011 *Chin. Phys. Lett.* **28** 120508
[20] Alasty A and Salarieh H 2007 *Chaos Soliton. Fract.* **31** 292
[21] Yau H T and Chen C L 2007 *Chaos Soliton. Fract.* **34** 1567
[22] Lin D, Wang X and Yao Y 2012 *Nonlinear Dynamics* **67** 2889
[23] Zhou J and Wen C 2008 *Adaptive Backstepping Control of Uncertain Systems* (Berlin, Heidelberg: Springer) pp. 9–31
[24] Swaroop D, Hedrick J K, Yip P P and Gerdes J C 2000 *IEEE Trans. Autom. Control* **45** 1893
[25] Park J H, Kim S H and Moon C J 2009 *IEEE Trans. Neural Netw.* **20** 1204
[26] Li Y, Qiang S, Zhuang X and Kaynak O 2004 *IEEE Trans. Neural Netw.* **15** 693
[27] Dawson D M, Carroll J J and Schneider M 1994 *IEEE Trans. Control Syst. Technol.* **2** 233
[28] Ioannou P A and Kokotovic P V 1984 *Automatica* **20** 583
[29] Wiggins S 1987 *Phys. Lett. A* **124** 138
[30] Hua C, Guan X and Shi P 2005 *Chaos Soliton. Fract.* **23** 757
[31] Levant A 2003 *Int. J. Control* **9** 924
[32] Khalil H K 1996 *IEEE Trans. Auto. Contr.* **41** 177
[33] Polycarpou M M 1996 *IEEE Trans. Auto. Contr.* **41** 447
[34] Sanner R M and Slotine J J 1992 *IEEE Trans. Neur. Netw.* **3** 837
[35] Wang H and Sun J 1992 *Proceedings of the* 31*st IEEE Conference on Decision and Control* 3255
[36] Wen C, Zhou J, Liu Z and Su H 2011 *IEEE Trans. Auto. Contr.* **56** 1672